Theoretical study of a body-centered-tetragonal phase of carbon nitride

Eunja Kim and Changfeng Chen
Department of Physics and High Pressure Science Center, University of Nevada, Las Vegas, Nevada 89154

Thomas Köhler, Marcus Elstner, and Thomas Frauenheim
Universitaet-GH Paderborn, Fachbereich Physik, Theoretische Physik, 33095 Paderborn, Germany
(Received 20 December 2000; published 13 August 2001)

We present the results of a theoretical study of a body-centered-tetragonal (BCT) phase of carbon nitride (CN) with 1:1 stoichiometry using a self-consistent-charge density-functional tight-binding method. This CN phase is highly stable and has a small c/a ratio of 0.34 with complicated N and C dimerization along the c axis. The N atoms form a quasi-one-dimensional polymeric chain structure. Bond lengths as short as 1.16 Å between C atoms and 1.11 Å between N atoms are obtained along the c axis. However, the bond lengths in the a-b plane are considerably longer, yielding only a modest bulk modulus of 243 GPa. We examine the structural and electronic properties to characterize and understand this CN phase.

DOI: 10.1103/PhysRevB.64.094107 PACS number(s): 61.50.Ah, 61.50.Ks, 61.50.Lt, 61.50.Nw

I. INTRODUCTION

Since the pioneering work by Cohen,[1] there has been considerable research interest in the search for new hard or low compressibility materials.[2,3] Although there has been no evidence so far for the existence of any material harder than diamond, the hardest material known, the theoretical and experimental attempts to construct new carbon and carbon nitride materials have led to many theoretical proposals and experimental discoveries of material structures with interesting electronic and structural properties. On the theoretical side, beside the various C_3N_4 phases proposed in earlier work[4,5] and extensively studied in subsequent research,[6–15] other crystalline carbon structures[16,17] and carbon nitride phases with 1:1 stoichiometry[18,19] and amorphous carbon nitrides[20] with a wide range of stoichiometries and densities have been investigated. On the experimental side, a lot of effort has been devoted to the synthesis and characterization of carbon nitrides in the C_xN_y phases.[21–31] Structural, electrical, mechanical, optical, and thermal properties of these phases have been extensively investigated. More recently, additional carbon nitride phases have been discovered in experiments. These include a fullereneslike,[32] a monoclinic,[33] a tetragonal,[34] and some other unknown phases in CN_x/TiN nanocomposite coatings[35] and CN_x/ZrN multilayers.[36] Amorphous C-N films also have been studied experimentally.[37–40]

The main interest in carbon and carbon-nitride materials stems from the belief that relatively short bond lengths and low bond ionicity in these materials make them primary candidates for low-compressibility or superhard materials.[2,3] An important consideration in these research activities is to use the increasingly powerful and reliable computational tools to explore and predict new material structures. In particular, since it is very difficult to grow single-crystal samples of these materials, most experimental results have resolutions too low to accurately identify the crystal structures and the internal atomic arrangement due to the limited quality of samples, and, therefore, theoretical calculations that can provide further details about the atomistic structure, stability, and related physical properties are highly desirable.

This work is motivated by recent experimental results[34] showing strong evidence for the existence of a carbon nitride phase with tetragonal symmetry and a stoichiometry close to CN(1:1). We have performed self-consistent-charge density-functional tight-binding total energy calculations to identify the tetragonal rocksalt crystal structure and internal atomic arrangement for this CN phase.[41] The calculated lattice constants and the c/a ratio of the tetragonal rocksalt phase of CN are in excellent agreement with experimentally measured values. In addition, we also have carried out a systematic study of cubic-to-tetragonal structural transitions in the carbon nitrides with 1:1 stoichiometry and have found a highly stable body-centered tetragonal (BCT) CN phase with complex nitrogen and carbon dimerization and the ordering of the nitrogen dimers in the form of a polymeric chainlike structure.

In this paper, we present the results of a detailed study of the structural and electronic properties of the BCT phase of CN. We examine the structural details such as the radial distribution function, the bond angle distribution function, the carbon and nitrogen dimerization, and the rotation and ordering of the nitrogen dimers. We also examine the bonding behavior in the BCT structure, and calculate the electronic band structure. The fully relaxed BCT phase of carbon nitride has a small c/a ratio of 0.34 and, consequently, bond lengths as short as 1.16 Å between carbon atoms and 1.11 Å between nitrogen atoms along the c axis. However, the bond lengths in the a-b plane are considerably longer, yielding only a modest bulk modulus of 243 GPa. Although this carbon nitride phase turns out not to be a superhard material, its complex internal atomic structure makes it a very interesting material with a nitrogen polymeric chain structure in resemblance to the so-called polymeric twofold-coordinated chainlike structure observed in a high-pressure phase of pure nitrogen.[45] The simulation results indicate that the BCT phase of CN with the small c/a ratio of 0.34 is also a high-pressure phase with compression required along the c axis.

In Sec. II, we present a brief review of the theoretical

approach and the simulation constraints. The calculated structural and electronic properties of the BCT phase of CN are reported and discussed in Sec. III, followed by a summary in Sec. IV.

II. THEORETICAL APPROACH

For the large-scale total-energy calculations of the many-atom structures, we use the recently developed self-consistent-charge density-functional based tight-binding (SCC-DFTB) scheme.[42–44] The method is derived from density-functional theory (DFT) by a second order expansion of the Kohn-Sham energy functional with respect to charge fluctuations $\delta n(\vec{r})$ relative to a reference density $n_0(\vec{r})$. Efficiently approximating the second order terms in the density fluctuations by a simple distribution of atom-centered point charges $\Delta q_I = q_I - q_I^0$, estimated within a Mulliken analysis, the 2nd-order Kohn-Sham energy reads

$$E_2^{\mathrm{DFT}} = \sum_i^{\mathrm{occ}} n_i \langle \Psi_i | \hat{H}_0 | \Psi_i \rangle + E_{\mathrm{rep}}[n_0] + \frac{1}{2} \sum_{I,J}^{N} \gamma_{IJ} \Delta q_I \Delta q_J . \tag{1}$$

While the first term represents the electronic band structure energy of the system with occupation numbers of single-particle states n_i, E_{rep} as a short-range repulsive two-particle interaction includes the ionic repulsion and the Hartree and exchange-correlation double-counting contributions. Both expressions are determined at the reference density n_0. Finally the third term explicitly accounts for the long-range interatomic Coulomb interactions between net point charges at different lattice sites and the onsite self-interaction contributions of the single atoms. The interaction integrals γ_{IJ} reduces to the Coulomb form for large distances, they incorporate screening effects for intermediate distances and approximate as onsite-terms γ_{II} the chemical hardness or Hubbard parameters of the single atoms.

Representing the single-particle electronic states within a minimal basis LCAO (linear combination of atomic orbitals) expansion $\Psi_i(\vec{r}) = \Sigma_\nu c_{\nu i} \varphi_\nu(\vec{r} - \vec{R}_I)$ and writing the effective potential $V_{\mathrm{eff}}(n_0(\vec{r})) = V_{\mathrm{ext}} + V_H[n_0] + V_{XC}[n_0]$ in H_0 as a superposition of atomic contributions, the variational minimization of the approximate Kohn-Sham energy $\delta E_2^{\mathrm{DFT}} / \delta \Psi_i^*(\vec{r}) = 0$ with the normalization constraint yields a set of Kohn-Sham equations

$$\sum_\nu^M c_\nu^i (H_{\mu\nu} - \varepsilon_i S_{\mu\nu}) = 0, \quad \forall \mu, i, \tag{2}$$

which are self-consistent in the Mulliken-charge distribution through the charge modification of the Hamiltonian matrix,

$$H_{\mu\nu} = \langle \varphi_\mu | \hat{H}_0 | \varphi_\nu \rangle + \frac{1}{2} S_{\mu\nu} \sum_K^N (\gamma_{IK} + \gamma_{JK}) \Delta q_K$$

$$= H^0_{\mu\nu} + H^1_{\mu\nu}, \quad \forall \mu \epsilon I, \nu \epsilon J. \tag{3}$$

Since we are further using a DFT-based two-center construction of Hamiltonian and overlap integrals $H^0_{\mu\nu} = H_{\mu\nu}(n^0)$, $S_{\mu\nu}$ as well as the repulsive interactions $E_{\mathrm{rep}}(n_0)$ versus distance,[43,44] the SCC-DFTB method combines the simplicity and efficiency of common nonorthogonal two-center tight-binding schemes with a considerably improved accuracy and chemical transferability. The carbon and nitrogen tight-binding parameters generated using this method have been thoroughly tested on various molecular, amorphous, and crystalline phases involving carbon and nitrogen with excellent results.[20,42–44]

The periodic boundary conditions are applied during the simulation of the crystal structures. A total of 128 atoms were used in the calculation. The energetic minimization of the structure is obtained at the Γ point by an optimization of the supercell and subsequent molecular-dynamics annealing simulations of the internal atomic coordinates. We also have performed the convergency test and have found that the 128-atom supercell produces satisfactory results for both the equilibrium volume and the cohesive energy.

III. SIMULATION RESULTS AND DISCUSSION

Following the successful structural identification[41] of the tetragonal rocksalt phase of CN observed in experiment, we have carried out a systematic study of the cubic-to-tetragonal structural transition in carbon nitrides with 1:1 stoichiometry and have found additional stable tetragonal CN phases. The most interesting case is the transition from the BCC to the BCT structure. In this paper, we present structural and energetic details associated with this transition to fully characterize this CN structure.

Figure 1 shows the fully relaxed BCT structure. It is obtained by compressing the BCC structure along the c axis while allowing a full optimization of the supercell. The static structural optimization procedure is followed by a long molecular dynamics annealing simulation for further relaxation of the internal atomic positions. The final structure is obtained by the steepest decent relaxation.[46]

The phase transformation from BCC to BCT structure is of a very high energy gain of 2.70 eV/atom. The cohesive energy of the BCT phase is 7.69 eV/atom, close to the value of 8.07 eV/atom for diamond calculated within the same method. This indicates high stability of the BCT structure. The structural optimization of the supercell initially causes a volume shrinkage from 7.45 Å^3/atom to 6.35 Å^3/atom, resulting in the phase transition from cubic to tetragonal symmetry with a c/a ratio of 0.49. This volume of the BCT phase of carbon nitride obtained from static supercell optimization alone is close to the value obtained in a previous work on the pure carbon bct-4 structure.[17] In the present work, we apply molecular dynamics annealing simulations to allow further relaxation of the internal atomic positions in the structure. Consequently, two adjacent nitrogen atoms come close to form a N-N dimer. These nitrogen dimers then rotate away from the c axis and form an ordered polymeric chainlike structure, resulting in additional structural and volume changes with alternating bond lengths of 1.11 Å and 1.15 Å for the N dimers and a reduced c/a ratio of 0.34. Due to a large expansion of the lattice constants in the a-b plane during the molecular dynamics simulation, the final

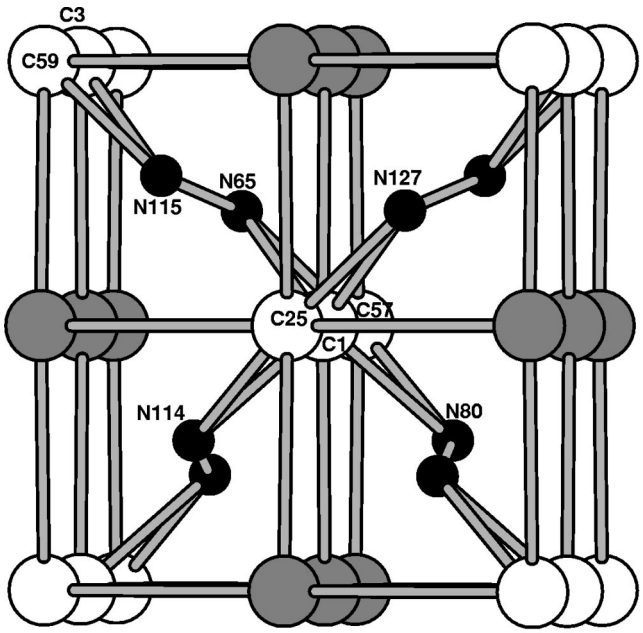

FIG. 1. The primitive cell of the fully relaxed BCT phase of CN. The black circles represent nitrogen atoms and the gray (open) circles represent carbon atoms with (without) dimerization along the *c* axis that points into the paper. The alternating bond lengths of the N dimers are 1.11 Å (attached to N65) and 1.15 Å (attached to N127). The C rows at the corner of the primitive cell have alternating bond lengths of 1.31 Å (between C59 and C3) and 1.37 Å, while those on the edge of the primitive cell have alternating bond lengths of 1.16 Å and 1.52 Å. The lengths of the bonds between a N atom and its first (N155−C59) and second (N155−C3) nearest C atoms are 2.46 Å and 2.60 Å. The bond length between the C atoms in the *a*-*b* plane is 3.96 Å. This structure has a C_2 symmetry.

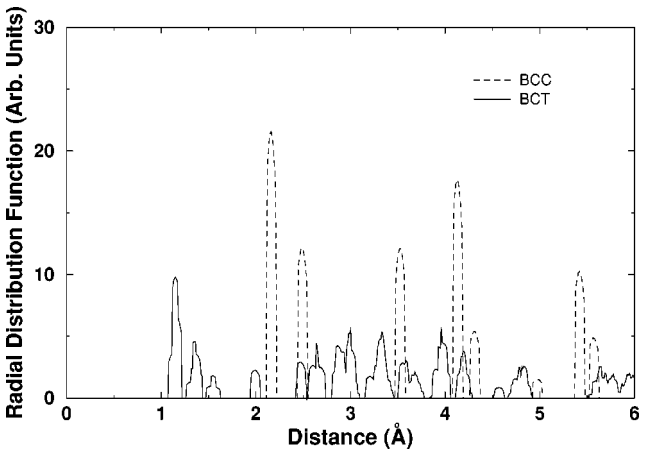

FIG. 2. Radial distribution function for the BCC and the BCT phase of CN. All the peaks in both cases have been identified. Those with small radial distances are specified as follows. The first peak in the BCC phase is contributed by the nearest C-N bonds and the second BCC peak is due to the nearest C-C bonds and the nearest N-N bonds. In the case of the BCT phase, the first peak is due to the C≡C triple bonds and the N=N double bonds, the second peak is due to the C=C double bonds, and the third peak the C-C single bonds.

equilibrium volume of the BCT phase increases to 10.9 Å/atom. It should be pointed out that there are several energy barriers[47] that have to be overcome in the simulation procedure at larger c/a ratios to reach the BCT structure with the c/a ratio of 0.34. This implies that experimental realization of the BCT phase of CN will require the application of pressure along the *c* axis.

To obtain a qualitative understanding of the structural transition from the BCC to the BCT phase, we examine the relative bond strength in these two phases. The bond energy sequence $E(\mathrm{N}{\equiv}\mathrm{N}){\geqslant}E(\mathrm{C}{\equiv}\mathrm{N}){\geqslant}E(\mathrm{C}{\equiv}\mathrm{C}){\geqslant}E(\mathrm{C}{=}\mathrm{C}){\geqslant}E(\mathrm{N}{=}\mathrm{N}){\geqslant}E(\mathrm{C}{=}\mathrm{N}){\geqslant}E(\mathrm{C}\text{-}\mathrm{C}){\geqslant}E(\mathrm{C}\text{-}\mathrm{N}){\geqslant}E(\mathrm{N}\text{-}\mathrm{N})$ is known for the CN systems.[48] In the BCC-to-BCT transition, energetically more favorable bonds are formed. To illustrate this point, we plot in Fig. 2 the radial distribution function of the BCC and the BCT structures. It is seen that there is a clear overall shift in the distribution function toward the small-distance side in the BCC-to-BCT transition. Contributions to all the peaks in the radial distribution function have been identified. Of particular interest is the observation that energetically more favorable C=C double bonds, C≡C triple bonds, and N=N double bonds are formed in the BCT phase whereas only weak single bonds exist in the BCC phase. We notice that the bond lengths of the N dimers in the BCT phase are very close to the value of 1.094 Å for isolated N_2 molecules.[49]

Another interesting issue is the role of the orientational ordering of N dimers in the structural transition. The rotation of the nitrogen dimers and the subsequent formation of the zig-zag N dimer chains are found to play an important role in further stabilizing the CN structure. We have studied several orientational configurations of the ordered nitrogen dimers in the BCT structure. Figure 3 shows three different configurations of the ordered nitrogen dimers. The most stable configuration shown in Fig. 3(c) has the nitrogen dimers pointing in different directions with a 0.18 eV/atom energy gain over the unrotated linear N dimer configuration. These N dimers form zig-zag polymeric chains along the *c* axis. It is noticed that the rotational ordering of the N dimers affect the energetics of the system by changing the local bonding environment but it does not cause any change in the volume or the c/a ratio.

In addition to the structural characterization presented above, we also have calculated the charge distribution and the electronic band structure of the BCT phase of CN. We first examine the charge distribution and the bonding characteristics. Figure 4 shows the contour plot of the valence charge density of the BCT phase in the [001] plane. It should be noticed that C atoms on the edge of the primitive cell (see Fig. 1) are out of the [001] plane due to a slight buckling of the C-C bonds resulted from the structural relaxation. As a result, only very low charge densities from these C atoms are projected onto the [001] plane. The top N atoms in the N dimers are also slightly out of the [001] plane with the down N atoms further away. However, since the π electrons on the N atoms are orientated along the *c* axis, their charge projection is stronger than those of the out-of-the-plane C atoms whose π electrons are orientated in the *a*-*b* plane. Since

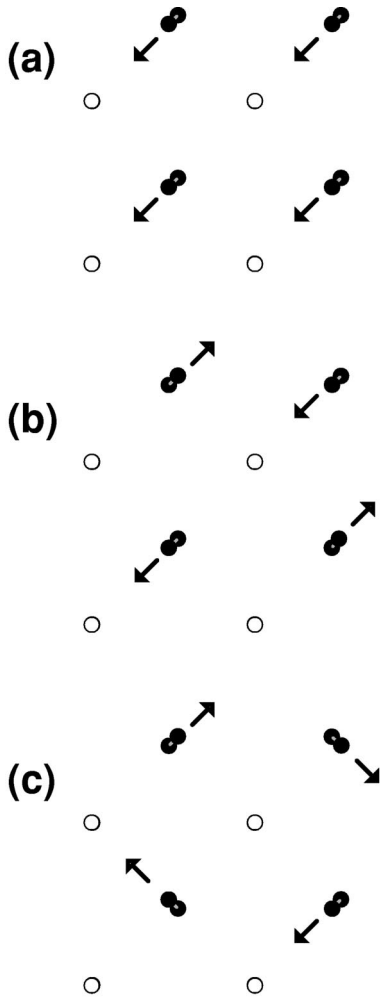

FIG. 3. Three configurations of the ordered nitrogen dimers in the BCT phase of CN with different N dimer rotation patterns. The arrows point from the down-atom toward the up-atom and indicate the orientation of the nitrogen dimers. The energy gains relative to that of the unrotated linear N dimer chain structure are (a) 0.10 eV/atom, (b) 0.04 eV/atom, and (c) 0.18 eV/atom. The black (open) circles represent nitrogen (carbon) atoms.

there is no high charge density contour between the C and the nearest N dimers, i.e., the charges are concentrated on the atoms not on the bonds, bonding in this BCT phase does not have a strong covalent character. However, it does show a unique bonding characteristic between a C atom and its nearest C atoms and two nearest N dimers. Each C atom makes not only four bonds with the nearest N dimers but also two other bonds with the nearest C atoms (out of the [001] plane and not shown in the figure), one strong double bond of length 1.31 Å with the up C atom and one weak double bond of length 1.37 Å with the down C atom. Overall, the C atom has two strong carbon bonds and four fairly weak C-N bonds in this configuration. The charge density of C atoms located at the corner and the center is fairly elliptically symmetric around the atoms, demonstrating sp-hybrid electrons of C atoms. The directional orientation of π electrons of the corner C atoms is perpendicular to that of the center C atom. Four π electrons of the N dimers also clearly appear in this

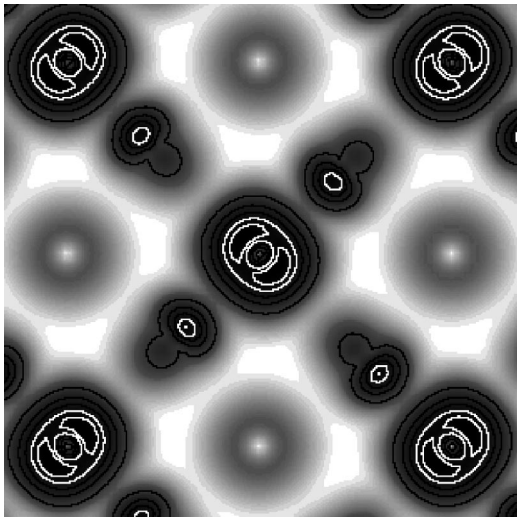

FIG. 4. The valence charge density plot for the BCT phase of CN in the [001] plane. The contour plot is in steps of 0.2 a.u. from 0.00 to 2.00 a.u. The black (white) area indicates higher (lower) electron density. The five big contours at the corner and center represent the valence charge density of C atoms. The four small contours between these C atoms represent the valence charge density of N dimers. There are four spherically symmetric images at the edge, coming from the out-of-the-plane C atoms as a result of the slight buckling of the C-C bonds after the structural relaxation. The gray areas between the C atoms and the neighboring N dimers indicate weak covalent bonding environment in the BCT phase of CN.

plot. Overall, the Jahn-Teller distortion is clearly seen in both C atoms and the N dimer. The bonding character of charges is quantitatively described by the percentage of the s character involved.[50] For the BCT phase the s character of carbon atoms is 29%, implying a hybridization between sp^2 and sp^3, while the s character of nitrogen atoms is 33%, indicating exactly sp^2 hybridization.

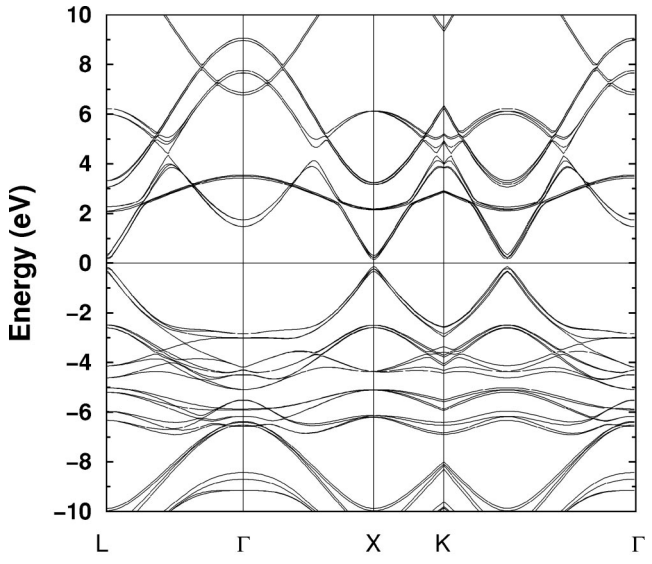

FIG. 5. Band structure for the BCT phase of CN. The Fermi energy is at $E=0$ eV.

Figure 5 shows the calculated electronic band structure of the BCT phase of CN. A small band gap of 0.12 eV is obtained. However, it should be noted that since a minimal LCAO basis is used in the present SCC-DFTB calculation, the value obtained here may represent an overestimate of the actual band gap. Given the small value of the calculated band gap, our results are inconclusive about the existence of a band gap in the BCT phase of CN.

IV. SUMMARY

We have carried out a theoretical study of a body-centered tetragonal phase of carbon nitride with 1:1 stoichiometry using a self-consistent-charge density-functional tight-binding method. Interesting structural features such as a small c/a ratio of 0.34 and complicated nitrogen and carbon dimerization along the c axis have been found. Very short bond lengths of the C and N dimers along the c axis combined with long bond lengths in the a-b plane yield a modest of bulk modulus of 243 GPa. This carbon nitride structure has a high cohesive energy close to that of diamond, indicating high stability. We also have examined the bond and charge distribution in the BCT structure and have calculated the electronic band structure. The short c axis in the structure is obtained only after several energy barriers have been overcome during the simulation process. It suggests that, unlike the recently discovered tetragonal rocksalt phase of CN which also has a small c/a ratio but does not encounter any energy barrier in reaching the equilibrium structure in the simulation, the formation of the BCT phase of CN will require applied pressure along the c axis. Experimental confirmation of this theoretically predicted structure will not only expand the family of carbon nitrides with tetragonal symmetry but also stimulate further exploration for different CN phases.

ACKNOWLEDGMENTS

This work was supported by DOE SPS and EPSCoR programs at UNLV and by DFG at Paderborn. Technical assistances by Michael Sternberg and Gerd Jungnickel are gratefully acknowledged.

[1] M.L. Cohen, Phys. Rev. B **32**, 7988 (1985); Nature (London) **338**, 291 (1989).
[2] M.L. Cohen, Mater. Sci. Eng., A **209**, 1 (1996).
[3] E.G. Wang, Prog. Mater. Sci. **41**, 242 (1997).
[4] A.Y. Liu and M.L. Cohen, Science **245**, 841 (1989).
[5] A.Y. Liu and M.L. Cohen, Phys. Rev. B **41**, 10 727 (1990).
[6] J.L. Corkill and M.L. Cohen, Phys. Rev. B **48**, 17 622 (1993).
[7] A.Y. Liu and R.M. Wentzcovitch, Phys. Rev. B **50**, 10 362 (1994).
[8] H. Yao and W.Y. Ching, Phys. Rev. B **50**, 11 231 (1994).
[9] J. Kouvetakis, A. Bandari, M. Todd, B. Wilkens, and N. Cave, Chem. Mater. **6**, 1376 (1994).
[10] T. Hughbanks and Y. Tian, Solid State Commun. **96**, 321 (1995).
[11] J. Ortega and O.F. Sankey, Phys. Rev. B **51**, 2624 (1995).
[12] A. Reyes-Serrato, D.H. Galvan, and I.L. Garzon, Phys. Rev. B **52**, 6293 (1995).
[13] D.M. Teter and R.J. Hemley, Science **271**, 53 (1996).
[14] A.T. Balaban, D.J. Klein, and W.A. Seitz, Int. J. Quantum Chem. **60**, 1065 (1996).
[15] J.V. Badding and D.C. Nesting, Chem. Mater. **8**, 535 (1996).
[16] A.Y. Liu, M.L. Cohen, K.C. Hass, and M.A. Tamor, Phys. Rev. B **43**, 6742 (1991).
[17] A.Y. Liu and M.L. Cohen, Phys. Rev. B **45**, 4579 (1992).
[18] M. Cote, J.C. Groosman, M.L. Cohen, and S.G. Louie, Phys. Rev. B **58**, 664 (1998).
[19] M. Cote and M.L. Cohen, Phys. Rev. B **55**, 5684 (1997).
[20] F. Weich, J. Widany, and T. Frauenheim, Phys. Rev. Lett. **78**, 3326 (1997).
[21] H.X. Han and B.J. Feldman, Solid State Commun. **65**, 921 (1988).
[22] C.M. Niu, Y.Z. Lu, and C.M. Lieber, Science **261**, 334 (1993).
[23] K.M. Yu, M.L. Cohen, E.E. Haller, W.L. Wansen, A.Y. Liu, and I.C. Wu, Phys. Rev. B **49**, 5034 (1994).
[24] T. Okada, S. Yamada, Y. Yakluchi, and T. Wada, J. Appl. Phys. **78**, 7416 (1995).
[25] Z.J. Zhang, S. Fan, and C.M. Lieber, Appl. Phys. Lett. **66**, 3582 (1995).
[26] T.Y. Yen and C.P. Chou, Appl. Phys. Lett. **67**, 2801 (1995); Solid State Commun. **95**, 281 (1995).
[27] J. Peng, Y.F. Zhang, S.Z. Yang, and G.H. Chen, Mater. Lett. **27**, 125 (1996).
[28] L.A. Bursill, J. Peng, V.N. Gurarie, A.V. Orlov, and S. Prawer, J. Mater. Res. **10**, 2277 (1995).
[29] Y. Chen, L.P. Guo, F. Chen, and E.G. Wang, J. Phys.: Condens. Matter **8**, L685 (1996).
[30] Y. Chen, L.P. Guo, and E.G. Wang, Mod. Phys. Lett. B **10**, 615 (1996); Philos. Mag. Lett. **75**, 155 (1997).
[31] S. Muhl and J.M. Mendez, Diamond Relat. Mater. **8**, 1809 (1999).
[32] H. Sjostrom, M. Stafstrom, and J.E. Sundgren, Phys. Rev. Lett. **75**, 1336 (1995).
[33] L.P. Guo, Y. Chen, E.G. Wang, L. Li, and Z.X. Zhao, Chem. Phys. Lett. **268**, 26 (1997).
[34] L.P. Guo, Y. Chen, E.G. Wang, L. Li, and Z.X. Zhao, J. Cryst. Growth **178**, 639 (1997).
[35] D. Li, X.W. Lin, S.C. Cheng, V.P. Dravid, Y.W. Chung, M.S. Wong, and W.D. Sproul, Appl. Phys. Lett. **68**, 1211 (1996).
[36] M. Wu, W. Qian, Y. Chung, Y. Wang, M. Wong, and W.D. Sproul, Thin Solid Films **308-309**, 113 (1997).
[37] C.S. Torng, J.M. Sivertsen, J.H. Jundy, and C. Chang, J. Mater. Res. **5**, 2490 (1990).
[38] D. Li, Y.-W. Chung, and W.D. Sproul, J. Appl. Phys. **74**, 219 (1993).
[39] D. Marton, K.J. Boyd, A.H. Al-Bayati, S.S. Todorov, and J.W. Rabalais, Phys. Rev. Lett. **73**, 118 (1994).
[40] Y. Yong, K.A. Nelson, and F. Adibi, J. Mater. Res. **10**, 41 (1995).
[41] Eunja Kim, Changfeng Chen, Thomas Köhler, Marcus Elstner, and Thomas Frauenheim, Phys. Rev. Lett. **86**, 652 (2001).
[42] D. Porezag, T. Frauenheim, T. Köhler, G. Seifert, and R. Kaschner, Phys. Rev. B **51**, 12 947 (1995).

[43] M. Elstner, D. Porezag, G. Jungnickel, J. Elstner, M. Haugk, and T. Frauenheim, S. Suhai, and G. Seifert, Phys. Rev. B **58**, 7260 (1998).

[44] T. Frauenheim, G. Seifert, M. Elstner, Z. Hajnal, G. Jungnickel, D. Porezag, S. Suhai, and R. Scholz, Phys. Status Solidi B **217**, 41 (2000).

[45] C. Mailhiot, L.H. Yang, and A.K. McMahan, Phys. Rev. B **46**, 14 419 (1992).

[46] M.C. Payne, M.P. Teter, D.C. Allan, T.A. Arias, and J.D. Joannopoulos, Rev. Mod. Phys. **64**, 1045 (1992).

[47] Due to extremely high computational cost, we did not search for the details of these energy barriers and the associated metastable phases. Instead, we just forced the change in the c/a ratio in the simulation in search for the eventual equilibrium structure.

[48] I. T. Millar and H. D. Springall, *A Shorter Sidwick's Organic Chemistry of Nitrogen* (Clarendon, Oxford, 1969), p. 16.

[49] G. Herzberg, *Spectra of Diatomic Molecules* (B. Van Nosirani, Princeton, NJ, 1950), p. 553.

[50] A. Streitweiser, Jr. and P. H. Owens, *Orbital and Electron Density Diagrams* (The Macmillan Company, New York, 1973), p. 29.